FULL LENGTH PAPER

SIMPLE MATHEMATICAL MODELS FOR THE DYNAMICS OF SPACECRAFT WITH DEPLOYED SOLAR PANELS

Thomas K Joseph; K. Renji
Structures Group
ISRO Satellite Centre (ISAC)
HAL Airport Road
Bangalore-560 017, India
Email : tkj@isac.gov.in; renji@isac.gov.in

Kartik Venkatraman
Department of Aerospace Engineering
Indian Institute of Science
Bangalore-560 012, India
Email : kartik@aero.iisc.ernet.in

Abstract

Most present day spacecrafts have large interconnected deployed solar panels having very low natural frequencies. The control torque applied to maneuver the spacecraft sets up transient oscillations in the spacecraft. The present work studies the nature of these interactions. The spacecraft in orbit can be modeled as a free rigid mass with flexible elements attached to it. It is shown that the oscillations of the spacecraft body are characterized by the dynamic characteristics of the flexible panel even if the mass and mass moment of inertia of the body is signifcantly higher than that of the flexible panels. A simple model consisting of an Euler-Bernoulli beam attached to a mass can represents such a system. The infuence of various parameters of the Euler-Bernoulli beam and the rigid element on the disturbances caused in the rigid element are investigated. The characteristics are determined for a step and also for a torque input. The responses are obtained in terms of nondimensionalised quantities. It is demonstrated that using the simple model developed the responses of spacecraft body can be easily obtained.

Key words*: Vibration, Transient response, On-orbit, Spacecraft*

Introduction

The escalation of power requirements in spacecraft has led to the design of large solar panels. Since these panels are very large they have to be stowed during launch and are deployed in orbit. The natural frequencies of the deployed solar panels are very low. In most of the present day spacecraft, the desired maneuver of the spacecraft is carried out by applying the required torque generated through changing the speed of the momentum wheels. But the low values of the natural frequencies pose difficulties in maneuvering the spacecraft. The control torque required is infuenced by the flexibility of the solar arrays. The maneuvering of the spacecraft produces transient oscillations of the main body and hence induce disturbances in the payload attached to it. In some specific applications these disturbances should be less than 5×10^{-5} degree. The issue becomes signifcant when one needs to maneuver the spacecraft quickly and needs to carry out the payload operations immediately.

The spacecraft in orbit can be considered as a free rigid element attached with large flexible panels. Several investigations have been carried out on the stabilization of the spacecraft after maneuver, assuming the satellite to be rigid. Nohmi and Uchiyama [1] used a simplified model of the spacecraft consisting of a rigid body and two flexible appendages. Using the satellite model which is a rigid central body with one or more flexible appendages, [2] studied the interaction of the control system and flexible panels during orbit transfer maneuver. A satellite model based on a flexible Euler-Bernoulli beam connected to a rigid core was analyzed by [3]. Using the assumed mode method, the equations of motion were derived and response of the system to the torque is obtained. Though there are many studies reported on the dynamic behavior

Paper Code : V66 N2/786-2014. Manuscript received on 22 Jun 2012. Reviewed, revised and accepted as a Full Length Contributed Paper on 28 Apr 2014

of the spacecraft in orbit, they focus on the interactions between the flexible array and the attitude control of the spacecraft. That is, the problem addressed is on the torque to be applied to maneuver the spacecraft in the presence of the flexible arrays. But studies on the response of the spacecraft main body and its transient decay due to the application of torque are seldom reported and this is addressed in this work.

A spacecraft in orbit with deployed solar array is represented by a free rigid mass attached with flexible panels. Response characteristics of the system for an applied torque are then obtained. It is shown that response of the rigid mass is very much influenced by the dynamics of the flexible panel. The above mathematical model is based on the finite element method. To study the characteristics of the system for its various parameters an analytical model is preferred. A free beam with mass and inertia at one end is used for this purpose. The beam represents the solar panel and lumped mass and inertia represents the spacecraft main body.

There are several studies reported on the dynamics of a cantilever beam. Natural frequencies of cantilever beams with tip mass was obtained by [4]. Exact frequency and normal mode shape expressions are derived for generally restrained Bernoulli-Euler beams with unsymmetrical translations and rotations at either end [5]. Rao and Mirza [6] obtained the eigen-frequencies and mode shape parameters for a wide range of restraint conditions for an Euler-Bernoulli beam. Bhat and Wagner [7] studied natural frequencies of a cantilever with tip mass whose center of mass is offset from the tip. The vibration problem of a beam with an arbitrarily placed concentrated mass and elastically restrained against rotation at either end was also studied [8]. The effects on the eigen-frequencies of the system on the ratios of the concentrated mass to the mass of the beam, stiffness of the end spring to the stiffness of the beam, and position of the mass to the total length of the beam have also been studied. The vibration response of a cantilever beam to a base excitation is obtained by To [9]. Though there are numerous publications on the dynamic behavior of a cantilevered beam, there is hardly any work reported on the dynamic response behavior of the system in which a flexible beam is attached to a free rigid mass and subjected to a torque.

In this work a simple model to represent the dynamic behavior of the spacecraft in the orbit is developed. It consist of a beam with tip mass and moment of inertia which is in free-free condition and subjected to torque. The response quantities are expressed in terms of the non-dimensional structural parameters so that these results can be used for any combination of structural parameters. Using this model dynamic behavior of the spacecraft body are characterized. It is then demonstrated for a spacecraft. In many practical examples, the flexible panels are present on both sides of the rigid element. In the present study, for the sake of simplicity, the beam is present only on one side of the rigid element. Similar results can be obtained for the system with two beams with a rigorous mathematical treatment.

Transient Response of Spacecraft Due to Torque

The spacecraft consists of two panels attached to the spacecraft main body as shown in Fig.1. The mass of the spacecraft body is 646.1 kg. The axis system is shown in Fig.2. The mass moments of inertia values are 212.2, 228.9 and 241.0 kg-m^2, respectively, about *X*, *Y* and *Z* directions. The mass and the mass moment inertia are lumped at the center of mass. The torque is applied about the *X*-axis.

The flexible element is an array of two panels. It consists of two rectangular panels each having dimensions 800 mm x 1450 mm. The panel is of sandwich construction and a schematic view is shown in Fig.1. The panel is connected to the spacecraft main body at two locations. Two stiffeners are provided on the panel near the fixing location to improve the bending sti?ness of the panel. Total mass of the panel is 13.9 kg.

The finite element (FE) model of the system is shown in Fig.2. The finite element model of the panel comprises of 8 noded shell elements. Spring elements are used to connect them. The mass of the system is 660 kg and the mass moments of inertia values are 246.1, 257.4 and 252.8 kg-m^2, respectively, about *X*, *Y* and *Z* directions.

Listed in Table-1 are the system and panel elastic modes. The system modes refer to the natural modes of the spacecraft with flexible solar panels. As such the first six system natural modes are the rigid body modes. The remaining are the system elastic modes. The panel elastic modes refer to the elastic modes of the solar panels when they are cantilevered. The first system and panel mode is the natural mode in bending of the panel and the second mode is the torsional mode. The bending mode of the system is shown in Fig.2. From Table-1, the system first and second mode frequencies are very close to the first two frequencies of the panel. This is because of the large mass and inertia of the spacecraft main body.

Table-1 : Natural Frequencies of the System

Mode	Natural Frequency (Hz)	
	System	Panel
1	6.69	6.34
2	10.22	10.17
3	17.06	15.95
4	26.79	26.09

The application of torque causes disturbance in the spacecraft. The equations of motions are

$$[M]\{\ddot{X}\} + [C]\{\dot{X}\} + [K]\{X\} = \{f(t)\} \tag{1}$$

The torque is applied about the X direction at the center of gravity of the spacecraft. In this case the center of gravity of the spacecraft is at the boundary of the system being analyzed. Since the force is applied at the boundary, the equations of motion can be partitioned as

$$\begin{bmatrix} M_{bb} & M_{bi} \\ M_{ib} & M_{ii} \end{bmatrix} \begin{Bmatrix} \ddot{x}_b \\ \ddot{x}_i \end{Bmatrix} + \begin{bmatrix} C_{bb} & C_{bi} \\ C_{ib} & C_{ii} \end{bmatrix} \begin{Bmatrix} \dot{x}_b \\ \dot{x}_i \end{Bmatrix}$$

$$+ \begin{bmatrix} K_{bb} & K_{bi} \\ K_{ib} & K_{ii} \end{bmatrix} \begin{Bmatrix} x_b \\ x_i \end{Bmatrix} = \begin{Bmatrix} F_b \\ 0 \end{Bmatrix} \tag{2}$$

Here b and i are the boundary and interior degrees of freedom respectively. Response in terms of displacement, velocities, and accelerations can be computed by solving Eq.(2).

We determined the response of the system to a unit step torque. A modal damping factor of 0.02 was used for the calculations. The angular displacement of the main body, without considering the rigid body modes, is shown in Fig.3. The frequency of the oscillation is about 6.5 Hz, which is the frequency of the fundamental mode of the system. As discussed earlier, in this case, it is very close to the fundamental frequency of the panel.

If the rigid body modes are included in the calculation, the angular displacement will tend to infinity. But the angular acceleration is expected to converge to the rigid body angular acceleration which in this case is 0.004147 rad/s^2. The angular acceleration of the spacecraft main body is determined and given in Fig.4.

A typical torque applied in practice is as shown in Fig.5. The torque is applied about X direction at the center of gravity of the spacecraft. The angular displacement of the main body about X without considering the rigid body modes is shown in Fig.6. The angular acceleration of the main body about X is calculated considering the rigid body modes. The response after 21 sec of the application of the load is shown in Fig.7. The angular acceleration of the main body, and hence the disturbances of the main body, show transient decay that corresponds to the mode of the flexible panel. It is expected that the transient decay will be at the frequency of the fundamental mode of the system. The result to be noted here is that though the rigid system has a very high mass and mass moment of inertia, the response of the rigid system is characterized by the dynamics of the flexible panels attached to it.

Simple Models for Dynamic Behavior

The results presented above are based on typical values for the structural properties of the system and it is based on finite element model. The characteristics for any other set of parameters can be obtained only by developing corresponding finite element model. Therefore suitable simple analytical model is preferred. The model considered here is an Euler-Bernoulli beam with a point mass and inertia attached at one end. The system is free in space. The beam represents the flexible panels and the lumped mass represents the rigid satellite body characterized in terms of its inertial mass and moments of inertia. The model is shown in Fig.8.

It is to be noted that the subject of interest is the response of the satellite body and not the panels. Therefore it is thought to be adequate to represent the panel by a beam representing the bending mode. Later the results will show that accurate results can be obtained using such models. If the dynamic responses of the panels are of interest then a 2D representation of the panels is necessary. The equations of motion of the system are presented first. Thereafter the natural frequencies of vibration together with the natural mode shapes of the system are determined. They are obtained for various values of normalized mass and mass moment of inertia. The transient response for a unit torque step function is determined. The variation in the time-domain response to various mass and mass moment of inertia ratios is studied to ascertain their effect.

Equations of Motion and Natural Modes

The beam has a flexural rigidity *EI*, mass per unit length m and length *L*. A mass M_0 having mass moment of inertia I_0 is attached to one end of the beam as shown in Fig.8. The equation of motion is then

$$EI\frac{\partial^4 \upsilon}{\partial x^4} + c\,\dot{\upsilon} + m\,\ddot{\upsilon} = f(x,t) \tag{3}$$

The boundary conditions at $x = 0$ are

$$EI\frac{\partial^2 \upsilon}{\partial x^2} = I_0\frac{\partial^3 \upsilon}{\partial x\,\partial t^2},\ EI\frac{\partial^3 \upsilon}{\partial x^3} = -M_0\frac{\partial^2 \upsilon}{\partial t^2} \tag{4}$$

and conditions that correspond to a free end are applied $x = L$.

The characteristic equation of the eigenvalue problem associated with Eq.(3) is obtained and variation of the displacement at a particular instant can be obtained as

$$\frac{d^4\phi(x)}{dx^4} = \lambda^4\phi(x), \tag{5}$$

where

$$\lambda^4 = \frac{m\omega^2}{EI} \tag{6}$$

Solution of Eq.(5) is of the form

$$\phi(x) = A\cos h\ \lambda x + B\sin h\ \lambda x + C\cos\ \lambda x + D\sin\lambda x, \tag{7}$$

where $\phi(x)$ is the eigen-function.

These boundary conditions at $x = 0$ and $x = L$ yield a set of four homogeneous equations in the four constants *A*, *B*, *C* and *D*. The matrix representation of the system of equations is

$$\begin{bmatrix} EI\lambda^2 & I_0\omega^2\lambda & -EI\lambda^2 & I_0\omega^2\lambda \\ -M_0\omega^2 & EI\lambda^3 & -M_0\omega^2 & -EI\lambda^3 \\ \cos h\,\lambda L & \sin h\,\lambda L & -\cos\lambda L & -\sin\lambda L \\ \sin h\,\lambda L & \cos h\,\lambda L & \sin\lambda L & -\cos\lambda L \end{bmatrix} \begin{bmatrix} A \\ B \\ C \\ D \end{bmatrix} = \begin{bmatrix} 0 \\ 0 \\ 0 \\ 0 \end{bmatrix} \tag{8}$$

which can be written as

$$\begin{bmatrix} 1 & \frac{Rr^3}{3} & -1 & \frac{Rr^3}{3} \\ -rU & 1 & -rU & -1 \\ \cos h\,r & \sin h\,r\,L & -\cos r & -\sin r \\ \sin h\,r & \cos h\,r & \sin r & -\cos r \end{bmatrix} \begin{bmatrix} A \\ B \\ C \\ D \end{bmatrix} = \begin{bmatrix} 0 \\ 0 \\ 0 \\ 0 \end{bmatrix} \tag{9}$$

The non-trivial solution is obtained by equating the determinant of the matrix in Eq. (9) to zero. That is

$$3 + r^4 RU + \cos h\,r\,((-3 + r^4 RU)\cos r + r(r^2 R + 3U)\sin r) + r(r^2 R - 3U)\cos r\sin h\,r = 0 \tag{10}$$

Here $R = \frac{3I_0}{mL^3}$ is the ratio of the mass moment of inertia of the right part to that of the flexible element and $U = \frac{M_0}{mL}$ is the ratio of the mass of the rigid part to that of the flexible element.

Equation (10) is a function of *r* and the roots of the equation are evaluated using Mathematica©. The lowest two roots are $r_1 = 0$ and $r_2 = 0$, which correspond to the rigid body modes of translation and rotation. $r_3 = \lambda_3 L$ is the first elastic mode frequency. Fig.9 shows the variation of r_3 for various values of mass ratio of the rigid part to the flexible element *U*, and mass moment of inertia ratio of the rigid part to the flexible element *R*. The results show that for large values of *U* and *R*, the natural frequency converges to the natural frequencies of the cantilevered beam. This is an expected result and it confirms the correctness of the present analysis. Also, these results help in obtaining the natural frequencies for any value of the structural parameter. Similar results are obtained for the other modes but not presented here. For each value of *r* the corresponding natural mode shapes are determined. The following expression gives the mode shape function.

$$\phi(x) = [(A(-(3+r^4 RU)\sin(r-\lambda x) + ((3-r^4 RU)\cos\lambda x - 6\,r\,U\sin\lambda x)\sinh r + \cosh\lambda x(-2r^3 R\cos r + (-3+r^4 RU)\sin r + (3+r^4 RU)\sinh r) + 3\cos r\sinh\lambda x - r\,U(r^3 R\cos r + 6\sin r)\sinh\lambda x + \cosh r(-2r^3 R\cos\lambda x + (-3+r^4 RU)\sin\lambda x - (3+r^4 RU)\sinh\lambda x)))/(-2r^3 R\cos r + (-3+r^4 RU)\sin r + (3+r^4 RU)\sinh r) \quad (11)$$

Figure 10 shows the first elastic mode shape of the beam for various values of ratios of mass and moment inertia of the rigid part to the flexible element. The results show that even for small values of U and R, the mode shapes converge to the mode shapes of the cantilever beam. For $U = 0$ and $R = 0$, the mode shapes are that of the free-free beam.

Similar curves can be obtained for other modes too, but not provided here for brevity. It is to be noted that the natural frequencies correspond to the beam with a mass and mass moment of inertia at the end and not with self mass alone. The end mass and moment of inertia are implicitly considered through boundary conditions. Hence these modes satisfy orthogonality.

Orthonormalization of Modes

The natural modes are orthogonal. Due to the presence of mass and mass moment of inertia at the end of the beam, the orthogonality relations for the modes get altered. It is to be noted that the orthogonality relation with respect to the stiffness does not get modified but the one with respect to the mass gets modified.

Let $\phi_i(x)$ and $\phi_j(x)$ be two different eigenfunctions of the system [10]. Using the integral calculus and applying boundary condition the orthogonality relation can be expressed as in Eq. (12).

$$\left[\int_0^L m\,\phi_j(x)\,\phi_i(x)\,dx + M_0\,\phi_j(0)\,\phi_i(0) + I_0\,\phi_j'(0)\,\phi_i'(0)\right] = 0\,,\ \omega_j^2 \neq \omega_i^2 \quad (12)$$

Orthonormalization of the right body modes requires some discussion. The rigid body modes can be shown to be of the form $\phi(x) = D_1 + D_2 x$. For the rigid body mode involving rigid translation, the eigen-function is A_1 and that involving rotation the eigen-function is $B_1 + B_2 x$. Since these modes should be orthonormal, we get

$$B_2 = \frac{-2B_1(mL + M_0)}{mL^2} \quad (13)$$

The two eigen-functions are

$$\phi_1(x) = A_1\,,\ \phi_2(x) = B_1\left[1 - \frac{2x(mL + M_o)}{mL^2}\right] \quad (14)$$

A_1 and B_1 can be determined by normalizing with respect to the mass

$$\int_0^L m A_1^2\,dx + M_0 A_1^2 = 1 \quad (15)$$

$$A_1 = \sqrt{\frac{1}{mL + M_0}} \quad (16)$$

$$\int_0^L B_1^2\left[1 - \frac{2x(mL + M_0)}{mL^2}\right]^2 m\,dx + M_0 B_1^2 + \frac{4I_0 B_1^2 (mL + M_0)^2}{(mL^2)^2} = 1 \quad (17)$$

$$B_1 = \sqrt{\frac{3m^2 L^4}{(mL + M_0)(12 I_0 (mL + M_0) + mL^3 (mL + 4M_0))}} \quad (18)$$

Nondimensionalized Response to Force Excitation

The equations of motion of the beam with a transverse vertically acting distributed force can be written as

$$EI\,\upsilon''''(x) + m\,\ddot{\upsilon}(x) = f(x, t) \quad (19)$$

The solution is of the form

$$\upsilon(x, t) = \sum_{i=1}^{\infty} a_i(t)\,\phi_i(x)\,, \quad (20)$$

where $a_i(t)$ is the generalized co-ordinate and $\phi_i(x)$ is the mode shape. Using the orthogonality relations, Eq. (12), the equation of motion of the beam with forcing term, Eq.(3) becomes

$$\ddot{a}_j(t) + \omega_j^2 a_j = p_j(t), \tag{21}$$

where $p_j(t) = \int_0^L f(x,t)\,\phi_j(x)\,dx$. Assuming modal damping for the system [11, 12], we can write the equations of motion for the damped case as

$$\ddot{a}_j(t) + 2\zeta_j \omega_j \dot{a}_j(t) + \omega_j^2 a_j(t) = p_j(t), \tag{22}$$

from which the response of the system in the generalized coordinate can be determined. Subsequently, using Eq.(20), the response of the system in the physical coordinates can be obtained. When a large number of variables are involved, non-dimensionalization of the parameters help in expressing the results. It also helps in avoiding computation for each new value of the physical parameter. Therefore some parameters as well as the response quantities are non-dimensionalized as described below. Let

$$\omega_c = \sqrt{\frac{EI}{mL^4}} \tag{23}$$

Dividing Eq. (22) by ω_c^2, we get

$$\frac{\ddot{a}_j(t)}{\omega_c^2} + \frac{2\zeta_j \omega_j \dot{a}_j(t)}{\omega_c^2} + \frac{\omega_j^2 a_j(t)}{\omega_c^2} = \frac{p_j(t)}{\omega_c^2} \tag{24}$$

Let $\tau = \omega_c t$ be the non-dimensionalised time and $\bar{\omega}_j = \frac{\omega_j}{\omega_c}$ be the non-dimensionalized natural frequencies. Defining $\bar{a}_j(t) = a_j(t)/L$, we obtain

$$\bar{a}_j''(\tau) + 2\zeta_j \bar{\omega}_j \bar{a}_j'(\tau) + \bar{\omega}_j^2 \bar{a}_j(\tau) = \frac{p_j(\tau)}{L\omega_c^2} = \bar{p}_j(t) \tag{25}$$

where $'$ denotes derivative with respect to non-dimensionalized time. Let $\bar{x} = \frac{x}{L}$ be the non-dimensionalized spatial coordinate and the modal vector can be written as $\phi_j(x) = \phi_j(\bar{x})$. The non-dimensional displacement response $\bar{\upsilon}(\bar{x}, \tau)$ is now

$$\bar{\upsilon}(\bar{x}, \tau) = \sum_{j=1}^{\infty} \bar{a}_j(\tau)\,\phi_j(\bar{x}) \tag{26}$$

The angular displacement is given by

$$\theta = \frac{d[\upsilon(x,t)]}{dx} = \frac{1}{L}\frac{d[\upsilon(\bar{x},\tau)]}{d\bar{x}} = \frac{d[\bar{\upsilon}(\bar{x},\tau)]}{d\bar{x}} \tag{27}$$

Hence the angular displacement in terms non-dimensionalized parameter is

$$\theta(\bar{x}, \tau) = \sum_{j=1}^{\infty} \bar{a}_j(\tau)\,\frac{d[\phi_j(\bar{x})]}{d\bar{x}} \tag{28}$$

Defining $\bar{\theta} = L\theta$, we get

$$\bar{\theta}(\bar{x}, \tau) = \sum_{j=1}^{\infty} a_j(\tau)\,\frac{d[\phi_j(\bar{x})]}{d\bar{x}} \tag{29}$$

Response to Unit Step Torque

Main interest of the present work is in the angular motion of the rigid system subject to a torque loading. An unit step torque is applied on the lumped mass and the responses are determined. The torque can be expressed in terms of the unit doublet function F_{-2}, which is given by [13].

$$F_{-2} = \langle x - a \rangle^{-2} \tag{30}$$

This function has the value 0 for $x \neq a$ and the value $\pm\infty$ for $x = a$. If the function given by Eq. (30) is multiplied by the torque value M, it represents the intensity of the equivalent distributed load. That is, the intensity of equivalent distributed load is $f(x, t)$.

$$f(x,t) = M \langle x - a \rangle^{-2} \tag{31}$$

from which the generalized force can be determined. Figs.11 to 13 show the non-dimensionalized angular displacements of the lumped mass for various values of U and R. Modal damping factor of 0.02 is considered for all the modes. The first three elastic modes are included in the response estimation but the rigid body modes are not included.

Table-2 : Frequency of Oscillation

System Parameter	Frequency of Oscillation	Natural Frequency
U = 20 R = 20	3.651 ω_c	3.650 ω_c
U = 40 R = 40	3.588 ω_c	3.584 ω_c
U = 80 R = 80	3.548 ω_c	3.550 ω_c

The angular displacements of the lumped mass show transient decay. The frequencies of these transient decays are given in Table-2 for various values of *U* and *R*. They are compared with the fundamental natural frequency of the system. It can be seen that the response of the lumped mass is a transient decay at the fundamental natural frequency of the system. It was shown earlier that the fundamental natural frequency of the system is governed by the fundamental natural frequency of the flexible panel. From these results one concludes that the response characteristic of the rigid element, though its mass and moment of inertia is very high, is very much influenced by the dynamics of the fundamental elastic mode of the flexible panel.

It is to be noted that the system has 6 rigid body modes and the seventh mode is the elastic mode. The transient decay will converge to the first elastic mode response. Hence the response seen is not rigid body motion but it is the elastic motion. During the elastic motion there is an angular displacement of the mass attached at the end causing the disturbances.

The angular displacement of the rigid element was computed and given for three values of *U* and *R*. Similar computations can be done for any value of *U* and *R*.

For a unit step torque, the angular acceleration should converge to zero if the rigid body modes are not included in the computation. Angular acceleration of the lumped mass for $U = 80$ and $R = 80$ is shown in Fig.14.

When the rigid body modes are included in the computation, the response should converge to the rigid body angular acceleration of the system, which is solely decided by the moment of inertia of the system. For a system having $U = 80$ and $R = 80$, the angular acceleration is expected to converge to $\frac{0.037}{m L^3}$. The response characteristic for $U = 80$ and $R = 80$ is shown in Fig.15.

All the above results confirm the correctness of the mathematical model, numerical computation of the response and the normalization procedure used.

Response to Torque Pulse

The responses are now obtained for a typical torque pulse applied in practice. A simplified form of such a typical torque pulse applied in practice is shown in Fig.16.

The response characteristics are expected to be dependent on the pulse width τ. Therefore it is convenient to non-dimensionalize the pulse width so that these results can be used for any other similar forcing functions. Define a parameter τ_n such that it is the ratio of pulse period to the natural period of the fundamental mode of the beam. A system with mass ratio $U = 80$ and mass moment of inertia ratio $R = 80$ and a modal damping factor of 0.02 is considered. Fig.17 show the non-dimensionalized angular displacement of the rigid element for various values of τ_n considering the first three elastic modes. Values of τ_n considered are 0.5, 1.0, 2.0 and 100. When τ_n is very large, that is the pulse width is very large compared to the natural period of oscillation, the response contains three transient decays. This is because the application of the positive torque produces a transient decay which is followed by the transient decay caused by the application of the negative torque. Lastly the torque becoming zero produces another transient decay. When τ_n is very small, that is the pulse width is very small compared to the natural period of oscillation, only one transient decay is seen. This is because by the time one oscillation is complete, the torque goes to a zero value. A similar results given in Fig.17(d) was obtained for a typical spacecraft as given in Fig.6. The simplified model is very much a representation of the problem in hand. For similar reasons, when τ_n is near unity, the response contains only one transient decay term. However, note that the response is quite significant when τ_n is near unity. The above results are for values of $U = 80$ and $R = 80$. Similar results can be obtained for any value of *U* and *R*.

Application to Spacecraft

The mathematical model developed in this work can be very easily used to estimate the disturbances caused to the spacecraft main body when it is subjected to a torque without using a finite element model. This is demonstrated for a spacecraft. The spacecraft considered in Section, Transient Response of Spacecraft due to Torque is consid-

ered here. Correspondingly following properties are used for the model. The mass of the beam is 13.7 Kg and length of the beam is 1.75 m. The cross section is selected such that the fundamental bending mode frequency of the beam is 6.44 Hz. It is to be noted that the beam represents the long flexible array and it has a natural frequency of 6.34 Hz as given in Table-1. The mass attached at the end is 646 Kg and the mass moment of inertia is 614 kg-m^2. These values correspond to those of the spacecraft body. The parameter mass ratio U is 46.5 and the inertia ratio R is 42.3. The first elastic mode is 6.44 Hz. The frequency of the spacecraft is 6.69 Hz.

The angular displacement of the end mass, that represents the spacecraft body, is obtained for a torque as given in Fig. 5. The computed angular displacement is shown in Fig.18. Comparing with the results of the spacecraft as given in Fig.6 it can be seen that the model developed predicts the spacecraft behavior very accurately.

Conclusion

Transient response of a spacecraft main body to the application control torque is studied. The results show that the transient disturbances of the free rigid elements are infuenced by the flexible element attached to it even though it is having very high mass and mass moment of inertia. A suitable simple analytical model that represent the dynamic behavior of the spacecraft body is developed. An expression for the response of the rigid element is derived. The transient decay of the rigid element is at the fundamental bending mode frequency of the beam. It is seen that response of the rigid element is significantly influenced by the dynamic characteristics of the beam. Response characteristics of the system for a torque pulse are then obtained. The dynamic disturbances are significant when the excitation pulse width is close to the natural period of the fundamental mode of the beam. Several results are provided in non-dimensionalized form using which the response of the rigid element can be directly obtained for any value of structural parameters and excitation pulse width. These results can be conveniently used to determine the transient oscillations of the main body of a spacecraft in orbit and subjected to a torque. This is demonstrated for a spacecraft. The model developed allows a quick and accurate estimation of responses.

References

1. Nohmi, M. and Uchiyama, M., "Dynamics and 3-Axes Control of a Spacecraft with Flexible Structures", Decision and Control, Proceedings of the 35th Conference on Decision and Control, Kobe, Japan, 1996, pp.2695-2700.
2. Silva, A.R. and De Souza, L.C.G., "Control System Flexible Satellite Interaction During Orbit Transfer Maneuver", Advances in the Astronautical Sciences, American Astronautical Society (AAS), 1998.
3. Trigolo, A., Kuga, H.K. and De Souza, L.C.G., "Parameter Identification of a Rigid-flexible Satellite Using Kalman Filter", Proceedings of the 17th International Congress of Mechanical Engineering.
4. Bhat, R. and Kulkarni, M.A., "Natural Frequencies of a Cantilever with Slender Tip Mass", AIAA Journal, 14, 1976, pp.536-537.
5. Register, A.H., "A Note on the Vibrations of Generally Restrained, End Loaded Beams", Journal of Sound and Vibration, 172, 1994, pp.561-571.
6. Rao, C.K. and Mirza, S., "A Note on Vibrations of Generally Restrained Beams", Journal of Sound and Vibration, 130, 1989, pp.453-465.
7. Bhat, B.R. and Wagner, H., "Natural Frequencies of a Cantilever with Tip Mass Slender in the Axial Direction", Journal of Sound and Vibration, 45, 1976, pp.304-307.
8. Goel, R.P., "Free Vibrations of a Beam-mass System with Elastically Restrained Ends", Journal of Sound and Vibration, 47, 1976, pp.9-14.
9. To, C.W.S., "Vibration of a Cantilever Beam with a Base Excitation and Tip Mass", Journal of Sound and Vibration, 83, 1982, pp.445-460.
10. Timoshenko, S., "Vibration Problems in Engineering", D Van Nostrand, 1964.
11. Clough, R.W. and Penzien, J., "Dynamics of Structures", McGraw-Hill, New York, U.S.A., 1993.
12. Meirovich, L., "Elements of Vibration Analysis", McGraw-Hill, New York, U.S.A., 1984.
13. Gere, J.M. and Timoshenko, S.P., "Mechanics of Materials", PWS Publishers, Boston, U.S.A., pp.389-405.

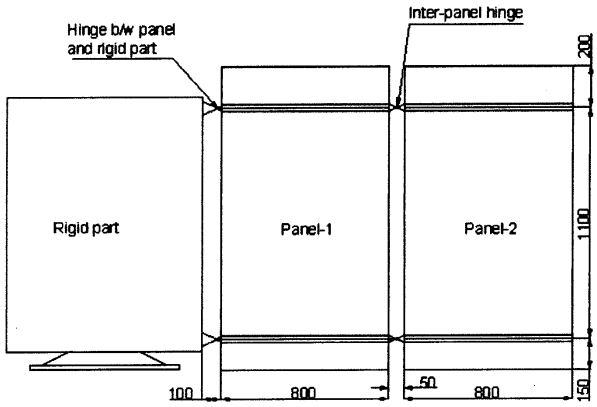

Fig.1 Schematic View of the System

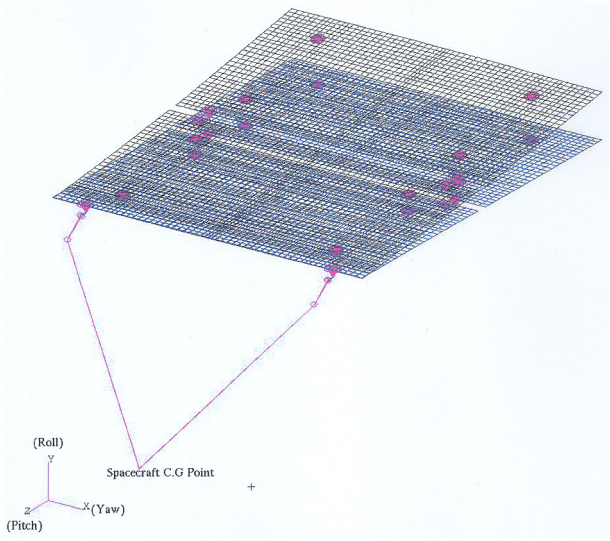

Fig.2 First Elastic Mode of the System in Free-free Condition

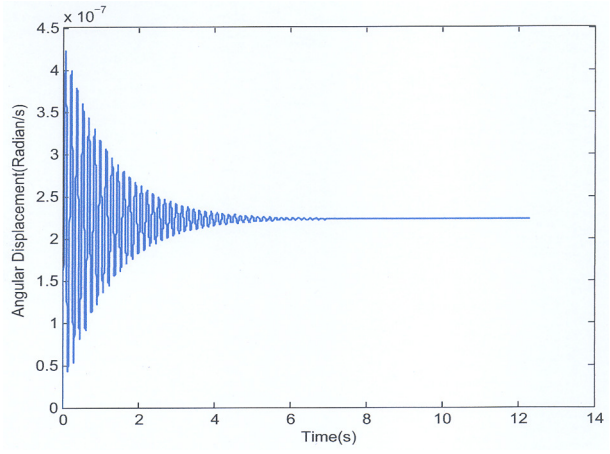

Fig.3 Angular Displacement of the Main Body for an Unit Step Torque

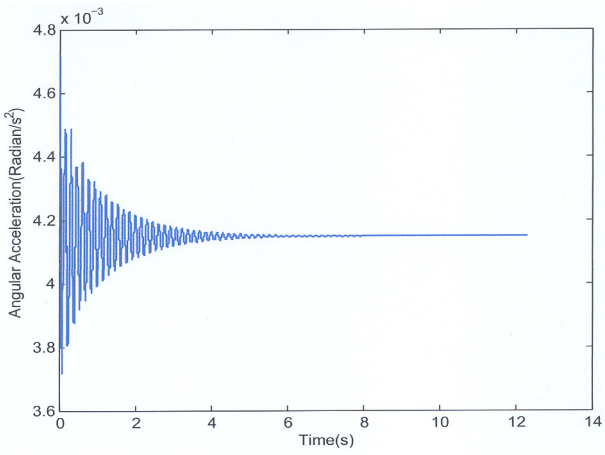

Fig.4 Angular Acceleration of the Main Body for an Unit Step Torque

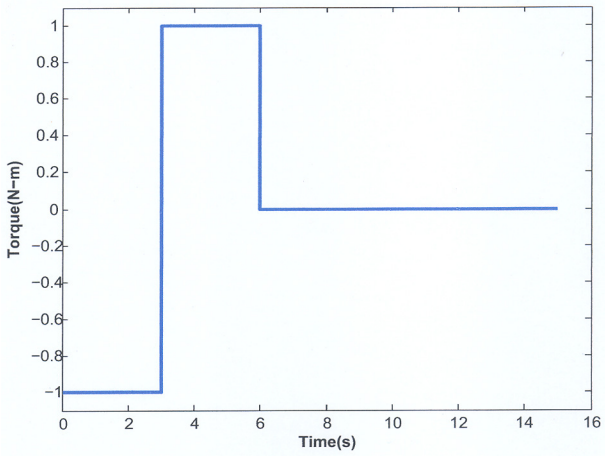

Fig.5 A Typical Torque Applied

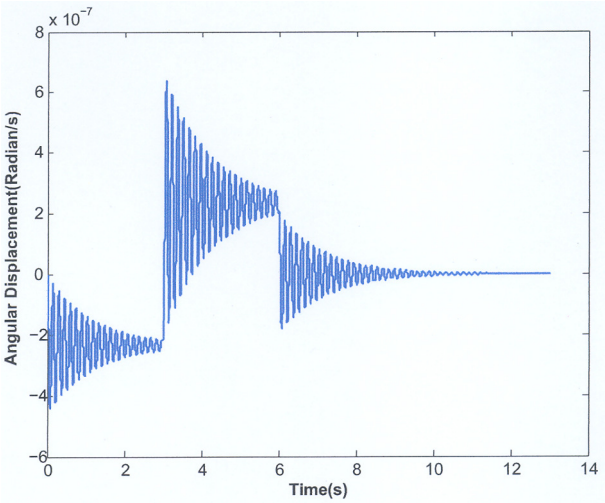

Fig.6 Angular Displacement of the Main Body Due to the Application of Typical Torque

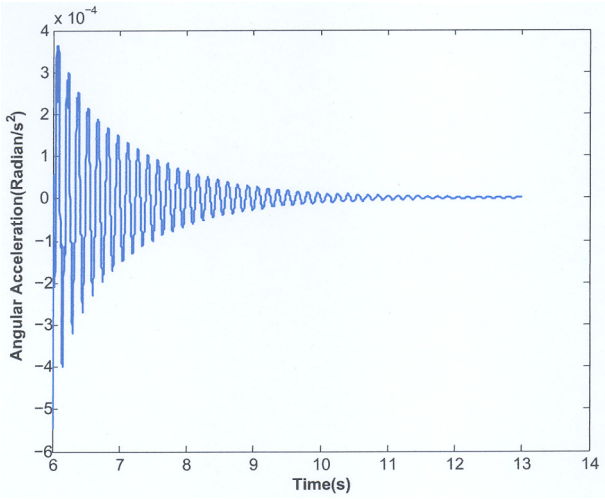

Fig.7 Angular Acceleration of the Main Body Due to the Application of Typical Torque

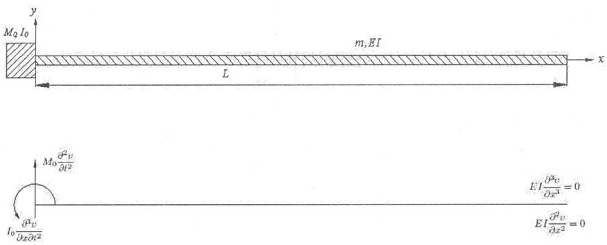

Fig.8 Euler-Bernoulli Beam Mounted on a Free Rigid System

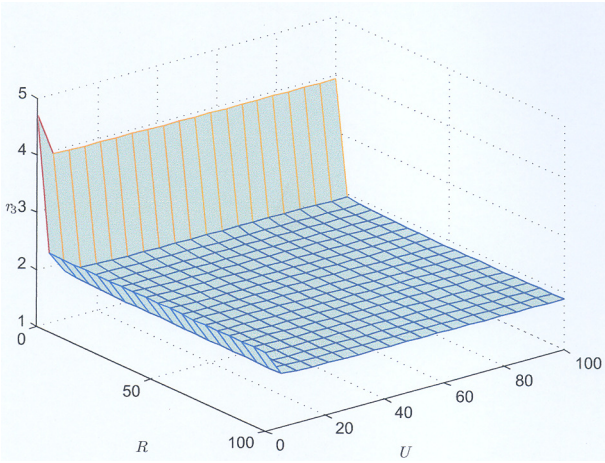

Fig.9 $r_3 = \lambda_3 L$ for Various Values of U and R

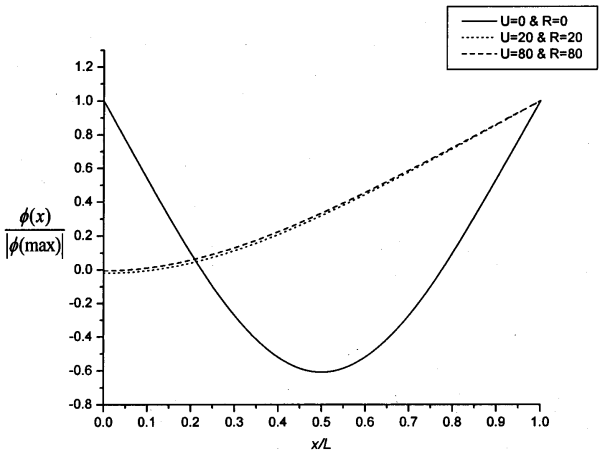

Fig.10 First Mode Shape

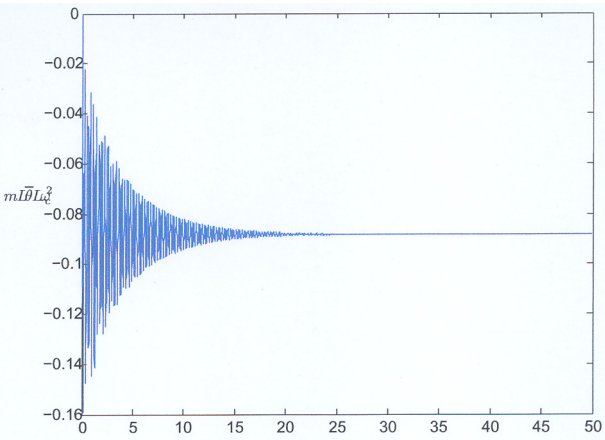

Fig.1 Angular Displacement of the Rigid Element for U = 0 and R = 0

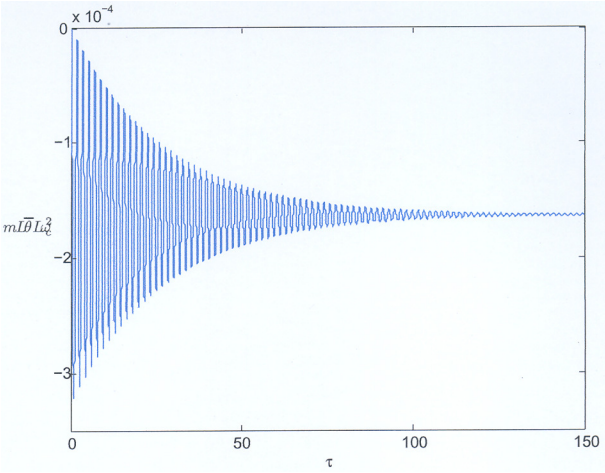

Fig.12 Angular Displacement of the Rigid Element System for U = 20 and R = 20

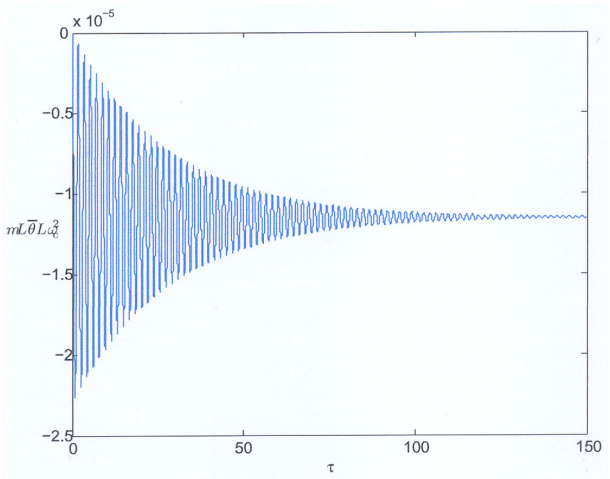

Fig.13 Angular Displacement of the Rigid Element for U = 80 and R = 80

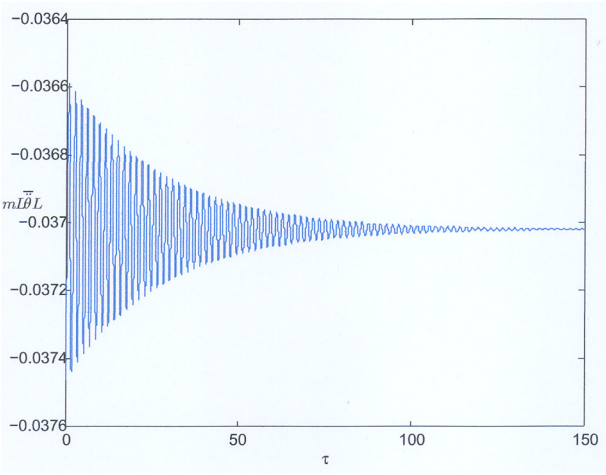

Fig.15 Angular Acceleration of the Rigid Element With Rigid Body Modes for U = 80 and R = 80

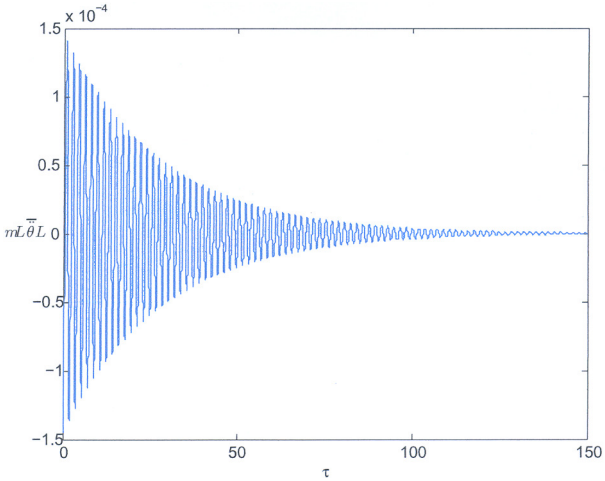

Fig.14 Angular Acceleration of the Rigid Element Without Rigid Body Modes for U = 80 and R = 80

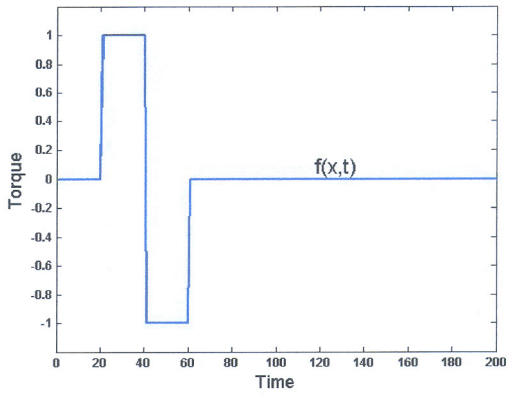

Fig.16 A Typical Torque Applied in Practice

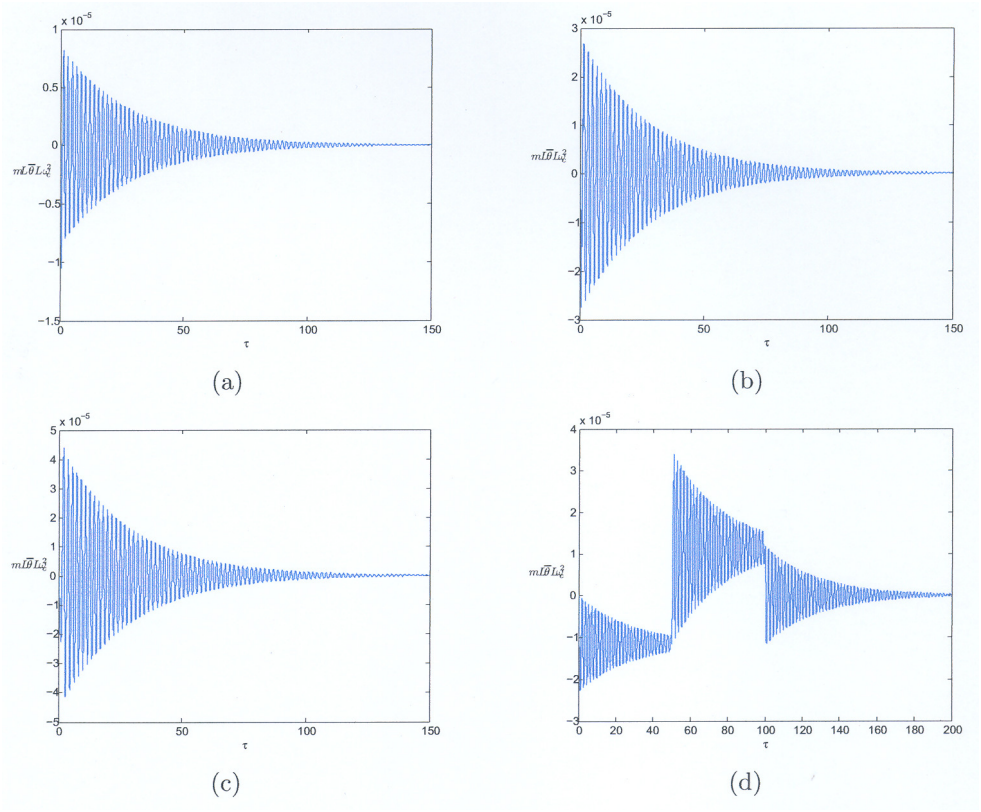

Fig.17 Non-dimensional Angular Displacement of the Rigid Element for Various Values of τ_n : (a) $\tau_n = 0.5$, (b) $\tau_n = 1$, (c) $\tau_n = 2$ and (d) $\tau_n = 100$

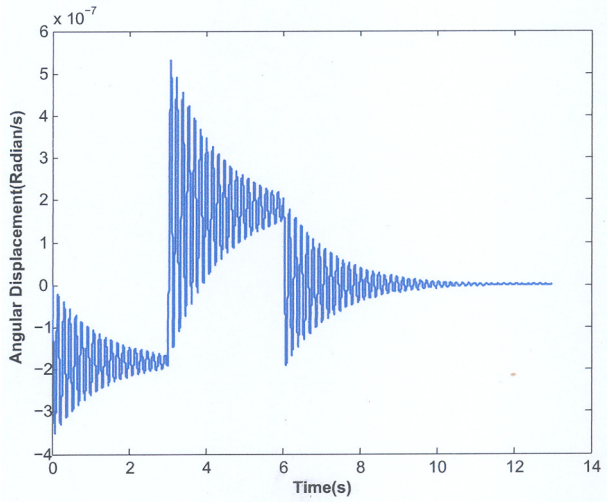

Fig.18 Angular Displacement of the End Mass Due to the Application of Typical Torque